

Microstructural Analysis of Barites Concrete

Bhagyamma G^a

^aResearch Scholar, Department of Civil Engineering,
Jawaharlal Nehru Technological University,
Ananthapuram, AP, India

Sri Chandana P^{b,*}

^{b,1}Department of Civil Engineering, Annamacharya
Institute of Technology and Sciences, Kadapa, AP, India.

Sudarasana Rao H^c

^cDepartment of Civil Engineering,
Jawaharlal Nehru Technological University, Ananthapuram, AP, India

Abstract— Alternate cementitious materials influence the formation of hydrate compounds through physical and chemical interactions with cement. Barites powder (BP) is one of the mineral material commonly used in concrete. In this paper, Cement was replaced by 0%, 5% and 20% of BP and a constant 1% of Titanium Dioxide (TiO₂) was used as an additive material. XRD technique, Scanning Electron Microscopy (SEM) and Energy Dispersive X-Ray (EDX) were used to study the chemical composition and morphology of concrete after 7 and 28 days of curing. The incorporation of barites powder and TiO₂ in concrete changed the cement hydration products, when compared to control mix and produces the CH crystals. The study shows the feasibility of using barites powder and TiO₂ in concrete.

Keywords— Barites powder, Titanium dioxide, Sustainable concrete, Compressive strength, morphology.

I. INTRODUCTION

Cement is the primary binding agent in concrete and is responsible for a substantial quantity of carbon dioxide emissions. Joseph Aspdin invented cement in 1824, and the Romans used it to construct concrete structures. Subsequently, people have attempted to enhance the properties of concrete by incorporating or modifying stone and non-stone materials [1, 2]. In recent years, the use of additives in concrete has been proposed to enhance the quality and environmental indicators and preventing pollution emissions to the atmosphere [2].

Barites powder is a naturally occurring mineral material, having high density that is abundantly available in many regions of Kadapa district, Andhra Pradesh, India. Due to its high density, it would be utilized in specialized concrete applications including high-density concrete and concrete that shields against radiation. In these applications, the high density of barite powder is used to provide additional radiation shielding or the use of nuclear technology requires the protection of living beings against the negative effects of radiation exposure. [3].

Numerous investigations showed that adding barite to concrete as an addition enhances its ability to attenuate gamma radiation [4-15]. Barite powder is typically used at replacement levels of 0-25% by weight of sand to improve the physical and mechanical properties of concrete including its elastic modulus, compressive strength, tensile strength,

density, shrinkage, and swelling, were compared to the results of a control mix. However, substitution of sand with barite powder has no negative effect on the compressive strength and swelling of concrete, but it decreases overall shrinkage [16].

Nano barite powder has been studied for its potential use as a supplementary cementitious material in concrete production [17]. Several studies shown that the addition of nano barite powder in concrete can enhance its mechanical properties, including compressive strength due to its higher surface area which allows better bonding with the cement matrix, resulting in an improved interfacial transition zone [2]. The replacement of various amounts of nano barite, ranging from 1% to 9% by weight of cement, was compared to the results of the control mix. The addition of 5% nano barites powder increases the compressive strength of concrete and 9% of Nano barite increases the performance of workability by 17% and also reduces the amount of water used in concrete samples [2]. It also influences the setting time of cement [18].

Barites powder and lime were typically used at replacement levels of 0 to 30% with an interval of 5%. The replacement of barites powder and lime with cement increases the compressive strength of concrete at 7 days of curing and which will be remains same for 14 days of curing for all the mixes but this effect does not show the improved results for 28 days of curing. The author highlighted that the replacement of barite with cement may produce better results than barites combined with lime [19].

Nano materials have an ability to accelerate the mechanical properties of concrete. From the previous studies, it is found that 1% of Nano Titanium dioxide (TiO₂) can increase the compressive, split tensile and flexural strengths concrete about 18%, 67% and 25% respectively, and water absorption was reduced by 3.68% when compared to normal concrete [20-23].

Recent studies provide insight into the use of barite as a replacement for fine and coarse aggregates. However, a limited works are available on the use of barite powder as a cement substitute material. Therefore, there is a growing interest in finding alternative materials that can be used as supplementary cementitious materials in concrete and that have good radiation ability. This study aims to investigate the microstructural properties which includes the morphology and chemical composition of concrete with barites powder used as a supplementary cementitious material and TiO₂ has been used as an additive to cement.

II. MATERIALS

In this study, an ordinary Portland cement of grade 53 was used. Barites powder with a particle of size ranging from 75µ to 100µ, was utilized. The test report obtained from X-ray

diffraction test was shown in Supplementary information Table-S1 [18]. River sand collected from the Penna River in Kadapa was used as a fine aggregate which conform to zone II. A Crushed granite stone of 20 mm size was used as coarse aggregate. A specific gravity of cement, barites, fine and coarse aggregates are 3.1, 4.1, 2.66 and 2.7 respectively [18]. A TiO2 of anatase type with a purity of 99% was used an additive in the concrete. The tap water was used for casting and curing. Conplast SP430 was used as a superplasticizer.

Table S1 Test Report of Barites Powder

Tests	Protocol	Results
Alumina as Al ₂ O ₃	IS 2881:1984 (Reaff:2003) by ICP OES	0.55%
Density	API Spec 13A Seventeenth Edition, November 2006 Errata, October 2008	4.200 g/cc
Iron as Fe ₂ O ₃	IS 2881:1984 (Reaff:2003) by ICP OES	0.51%
Residue greater than 75 µ	API Spec 13A Seventeenth Edition, November 2006 Errata, October 2008	1.15%
Soluble Carbonates	SGS/IN/CHML/MIN/SOP-01	1025 mg/kg
Soluble Sulphides	SGS/IN/CHML/MIN/SOP-02	48 mg/kg
Water soluble Alkaline Earth Metals as Calcium	API Spec 13A Seventeenth Edition, November 2006 Errata, October 2008	48 mg/kg
Total Barium as BaSO ₄	IS 2881:1984(Reaff:2003)	90.11%
Silica as SiO ₂	IS 2881:1984(Reaff:2003)	5.30%

III. METHODOLOGY

Barites concrete samples of size 150mm X150 mm X150mm were designed as per IS 519-1959, IS 10262-2009 and IS 456-2000 [24-26] with 1% of TiO2 for various percentages of barites powder, based on trial mixes the optimum dose of super plasticizer was obtained and used as 1%. These mixtures were designated as BC0, BC5, BC20 and

BT5, BT20 respectively, shown in Table-1. After 7 days and 28 days of curing the samples were tested for their microstructure characterization using SEM and EDX techniques.

Table 1 Mix designations

2	BC5	95	5	0
3	BC20	80	20	0
4	BT5	95	5	1
5	BT20	80	20	1

IV. RESULTS AND DISCUSSIONS

A. XRD Results

The X-ray diffraction analysis was performed to study the hydration compounds of cement for the control mix after 7 and 28 days of curing, shown in Fig 1. The graph shows the relation between intensity of the X-ray light, scattered from the collected sample and the angle difference of deflected x rays [27]. Sharp peaks were observed for the sample cured for 28 days than the 7 days of curing. It shows the crystalline phase of the material.

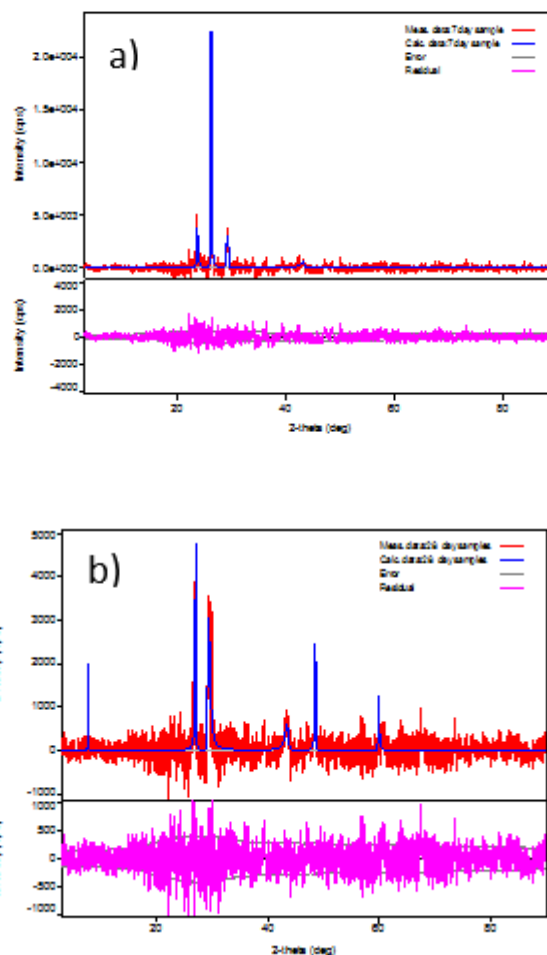
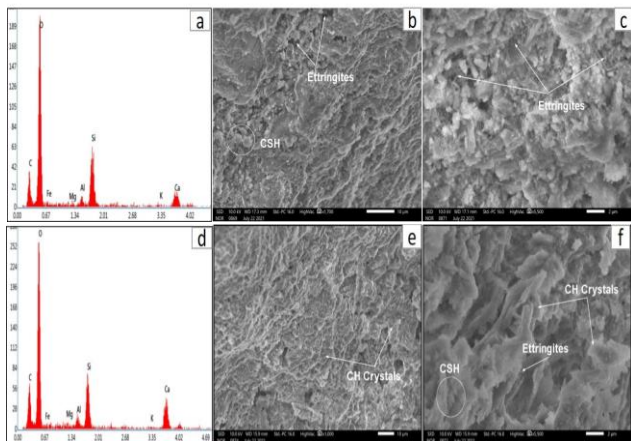


Fig 1. XRD pattern of control mix

a) After 7 days of curing b) 28 days of curing

B. SEM and EDAX Results

SEM and EDX techniques were employed to study the microstructural properties of concrete. The EDX represents the elemental composition of hydration products and SEM images



were analyzed for BC0, BC5, BC20, BT5, BT20 specimens after 7 days and 28 days of curing.

Fig. 2 EDX and SEM image of BC0 concrete, a) EDX pattern after 7 days of curing b) SEM image after 7days of curing c) Close-up of Etringite after 7 days of curing d) EDX pattern after 28 days of curing e) SEM image after 28 days of curing f) Close-up of CH crystals after 28 days of curing.

Sharp peaks of O, Si, C and small amount of Ca, Al were observed after 7 days of curing (Fig.2a). Needle like ettringites, CSH gel with sponge like structure were observed (Fig.2b). The needles of ettringites were developed in the pores, which controls the setting time of cement [28, 29] and its magnified view is shown in Fig.1c. Sharp peaks of O, Si, C and a wide distribution of Ca, Al were observed (Fig.2d) after 28 days of curing. The atomic percentage of Ca and C was more when compared to 7 days of curing. A developed hydrated C-S-H gel was produced (Fig.2e) due to an extended curing period of 28 days, which is responsible for the development of strength and durability of concrete [28, 29]. CH crystals and a small amount of ettringites were also developed, which can be seen in high magnified image (Fig.2f).

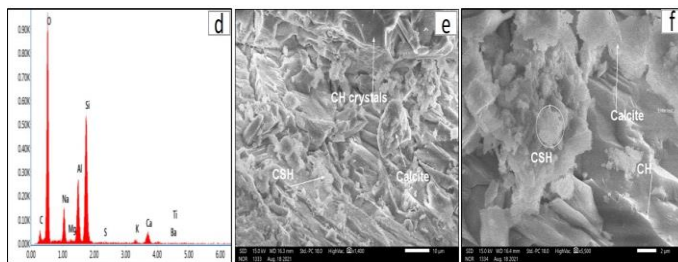
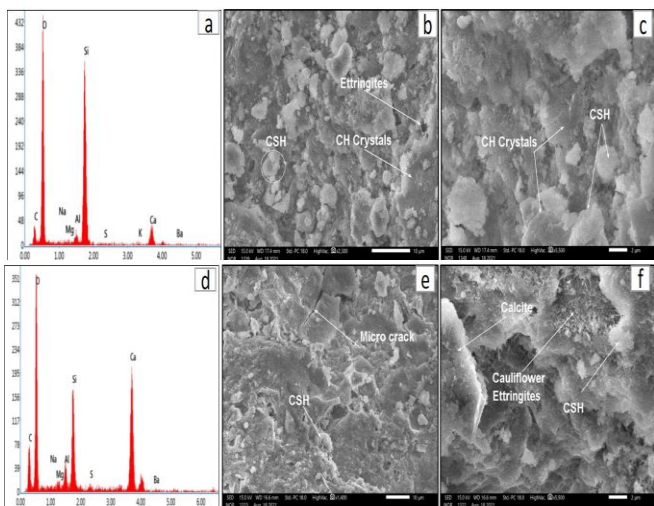
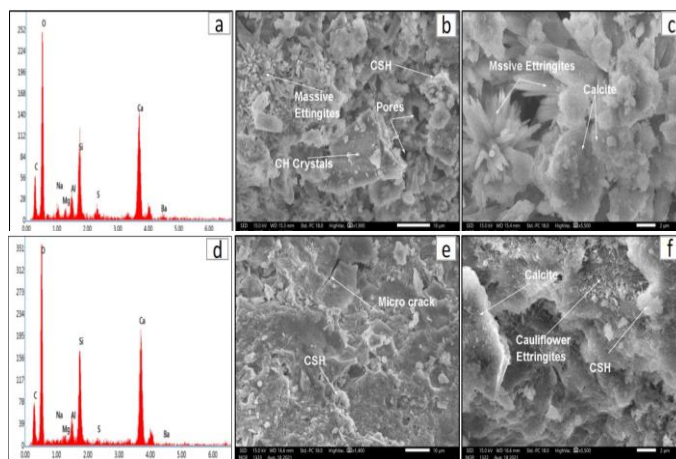


Fig. 3 EDX and SEM image of BC5 concrete, a) EDX pattern after 7 days of curing b) SEM image after 7days of curing c) Close-up of CSH and CH after 7 days of curing d) EDX pattern after 28 days of curing e) SEM image after 28

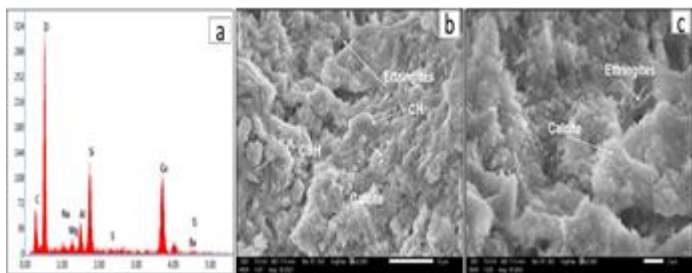


days of curing f) Close-up of Massive Etringite/ Cauliflower structure after 28 days of curing

Sharp peaks of O, Si, and small amounts of Ca, C, Al were observed after 7 days of curing (Fig. 3a). The atomic percentage of Si was more when compared to control mix of 7 and 28 days of curing. More Si in cement will increase the strength of cement. CH crystals, a tiny ettringite needles and CSH gel were observed in Fig. 3b. A clear image of sponge like CSH gel and CH crystals. Can be seen in high magnified image, shown in Fig.3c. Sharp peaks of O, Si, Al and small intensities of Ca, C, Al, S were observed after 28 days of curing. A massive ettringite or cauliflower structure was produced and encircled by hydrated CSH (Fig.3e). A clear view of ettringite needles were shown in high magnified image (Fig.3f), formation of ettringite leads to micro pores in the concrete that affects the strength of concrete.

Fig.4 EDX and SEM image of BC20 concrete, a) EDX pattern after 7 days of curing b) SEM image after 7days of curing c) close-up of massive ettringite and calcite after 7 days of curing d) edx pattern after 28 days of curing e) sem image after 28 days of curing f) close-up of massive ettringite/cauliflower structure after 28 days of curing.

Various peaks of O, Si, Ca, C, Al and S were observed (Fig.4a) after 7 days of curing and 28 days of curing (Fig.4a and 4d). The atomic percentage of Ca, C and Al was high as compared to control mix, shown in Fig 4a. Massive ettringite or cauliflower structure, Calcite and micro pores were



developed (Fig.4b). A closed image of massive ettringite was shown in Fig.4c, which are responsible for the formation of micro cracks. A close up of Massive ettringite and calcite after 28 days of curing was shown in Fig. 4f and is surrounded by calcite (because calcites are formed due to presence of calcium compounds, and calcites and ch crystals are having same structure).

Fig.4 EDX and SEM image of BC20 concrete, a) EDX pattern after 7 days of curing b) SEM image after 7days of curing c) Close-up of massive Ettringite and calcite after 7 days of curing d) EDX pattern after 28 days of curing e) SEM image after 28 days of curing f) Close-up of Massive Ettringite/ Cauliflower structure after 28 days of curing

Various peaks of O, Si, Ca, C, Al and S were observed (Fig.4a) after 7 days of curing and 28 days of curing (Fig.4a and 4d). The atomic percentage of Ca, C and Al was high as compared to control mix, shown in Fig 4a. Massive ettringite or cauliflower structure, Calcite and micro pores were developed (Fig.4b). A closed image of massive ettringite was shown in Fig.4c, which are responsible for the formation of micro cracks. A close up of Massive ettringite and calcite after 28 days of curing was shown in Fig. 4f and is surrounded by calcite (because calcites are formed due to presence of calcium compounds, and calcites and ch crystals are having same structure).

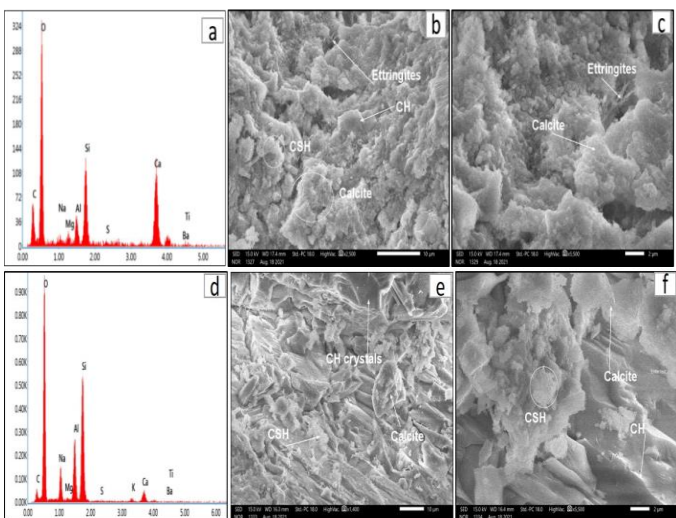


Fig. 5 EDX and SEM image of BT5 concrete, a) EDX pattern after 7 days of curing b) SEM image after 7days of curing c) Close-up of massive Ettringite and calcite after 7 days of curing d) EDX pattern after 28 days of curing e) SEM image

after 28 days of curing f) Close-up of CH and Calcite after 28 days of curing.

Strong peaks of O, Si, Ca, C, Al and some elements like T, S were observed (Fig.5a) after 7 days of curing CSH gel, small amounts of needle like ettringites, and calcite were observed in Fig.5b. A magnified view of ettringite and calcite was shown in Fig.5c. The combination of calcium and carbon results in the formation of calcium carbonate. Sharp peaks of O, Si, Al, Na and a small amount of Ca and C were observed in Fig.5d after 28 days of curing. The atomic percentage of Si and Al is high when compared to control mix. Hydrated CSH gel and CH crystals were observed in Fig.5e and 5f. Presence of TiO2 particle in cement can make the hydration products more reactive due to its more specific surface area [30].

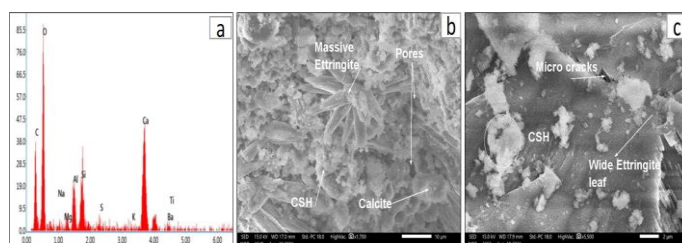
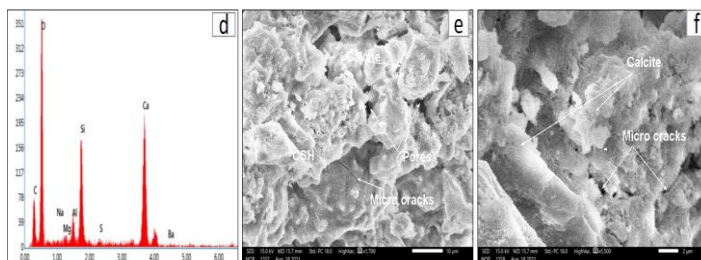


Fig. 6 EDX and SEM image of BT20 concrete, a) EDX pattern after 7 days of curing b) SEM image after 7days of curing c) Close-up of micro crack and wide Ettringite leaf after 7 days of curing d) EDX pattern after 28 days of curing e) SEM image after 28 days of curing f) Close-up of Calcite and micro cracks after 28 days of curing

Strong peaks of O, Si, Ca, C and narrow peaks of Al, S were observed in Fig.6a after 7 days of curing. The atomic percentages of Ca, C and Al were increased as compared to control mix, which are responsible for the development of calcite and ettringites. CSH gel, micro pores and massive ettringites or cauliflower structure were observed in Fig.6b. A close up of ettringites was shown on high magnified image, which illustrates the wide leaf(Cauli flowered structure) like ettringite formation, with micro crack. Various peaks of O, Si, C, and Ca were observed (Fig.6d) after 28 days of curing. Calcite, CSH gel, micro cracks and pores were observed in Fig.6e. A magnified view of crack can be seen in Fig 6f. As per the findings of some researchers, the expansion in the concrete is mainly due to delayed formation of ettringite which leads to its subsequent expansion and cracking [31]. Others states that the post ettringite deposition inside cracks or expansive gaps are caused by nucleation of ettringites in the crack tip zone [31-35] or by the hydraulic pressure caused by osmosis [35, 36]. Hence, these cracks were developed due to

formation of ettringites in the micro pores, which expands the cement by later precipitation.

CONCLUSION

Based on the results obtained the following conclusions were drawn.

- From the micro structural analysis, it can be concluded that more atomic percentage of Si was produced for BC5 concrete, attributes to the formation of CSH and hydrated CH crystals. Besides this, with an increase of barites powder and addition of TiO₂ particles ettringites needles were developed in the pores due to the formation of Al and S compounds, results in the formation of micro cracks.

- Mixture BC5, containing barites powder in concrete shows the early hydration process. Which indicates the good response of barites powder in concrete at this level when compared to control mix.

Authors' contributions

All the authors have contributed extensively to this manuscript. BG- experimentation, Methodology, analysis, Writing and curation of the work. SCP- Supervision, Conceptualization, Curation, Reviewing. SRH- Conceptualization, Reviewing, visualization.

DECLARATIONS

Conflict of interest The authors state that they do not have any competing interests, no financial support was received from any organization for the preparation of this manuscript.

References

- Neville, A. M.; Brooks, J.J., "Concrete Technology ", Pearson education Publication, 2nd Edition (2010).
- Ali Akbar Roshanasan and Javad Nasiri Rajabli, The Effect of Nano Barite Powder on Compressive Strength of Concrete and its effect on environment pollution, International Journal of Mechanical Engineering, 7(5) 0974-5823(2022).
- Shalbi, S., Sazali, N., Rosdi, M. A. A., & Idris, F. M., Study on mechanical and shielding properties of barite colemanite concrete. IOP Conference Series: Materials Science and Engineering, 1106(1) 012009(2021).
- Martin J E, Radiation Shielding in physics for radiation protection, Wiley-VCH Verlag GmbH, 367-423(2008).
- Shalbi, S., Sazali, N., Rosdi, M. A. A., & Idris, F. M., Study on mechanical and shielding properties of barite colemanite concrete. IOP Conference Series: Materials Science and Engineering, 1106(1) 012009(2021).
- Saidani, K., Ajam, L., & Ben Ouezdou, M., Barite powder as sand substitution in concrete: Effect on some mechanical properties. Construction and Building Materials, 95, 287–295, (2015).
- Bhruguli Gandhi, Review paper on use of barite powder in concrete, International Journal for Technological Research in Engineering, 5(9) 2347 – 4718(2018).
- I. Akkurt, H. Akyildirim, B. Mavi, S. Kilincarslan, C. Basyigit, Gamma-ray shielding properties of concrete including barite at different energies, Prog. Nucl. Energy 52, 620–623 (2010).
- S. Kilincarslan, I. Akkurt, C. Basyigit, The effect of barite rate on some physical and mechanical properties of concrete, Mater. Sci. Eng., A 424 (1–2) 83–86, (2006).
- K. Sakr, E. EL-Hakim, Effect of high temperature or fire on heavy weight concrete properties, Cem. Concr. Res. 35, 590–596 (2005).
- G. Gunduz, Colemanite–baryte frit and polymer impregnated concrete as shielding materials, Nucl. Eng. Des. 72, 439–447 (1982).
- I. Akkurt, A.M. El-Khayatt, The effect of barite proportion on neutron and gamma-ray shielding, Ann. Nucl. Energy 51, 5–9 (2013).
- E. Yilmaz, H. Baltas, E. Kiris, I. Ustabas, U. Cevik, A.M. El-Khayatt, Gamma ray and neutron shielding properties of some concrete materials, Ann. Nucl. Energy 38 2204–2212 (2011).
- I. Akkurt, I.C. Basyigit, C.S. Kilincarslan, B. Mavi, The shielding of gamma-rays by concretes produced with barite, Prog. Nucl. Energy 46, 1–11 (2005).
- F. Demir, G. Budak, R. Sahin, A. Karabulut, M. Oltulu, A. Un, Determination of radiation attenuation coefficients of heavyweight- and normal-weight concretes containing colemanite and barite for 0.663 MeV c-rays, Ann. Nucl. Energy 38 ,1274–1278 (2011).
- Saidani, K., Ajam, L., & Ben Ouezdou, M. (2015, October). Barite powder as sand substitution in concrete: Effect on some mechanical properties. Construction and Building Materials, 95 (2015) 287–295.
- Ali Akbar Roshanasan and Javad Nasiri Rajabli, The Effect of Nano Barite Powder on Compressive Strength of Concrete and its effect on environment pollution, International Journal of Mechanical Engineering, ISSN: 0974-5823, Vol. 7 No. 5 May, 2022.
- Bhagyamma G, Sri ChandanaPanchangam, Sudarsana Rao H, Development of self-cleaning cement mortar exposed to indoor and outdoor environment. Materials Today: Proceedings, (2023).
- P.Meenakshi, Partial Replacement of Cement by Barites and Lime Powder in Concrete, International Journal of ChemTech Research, 10 (3) ,143-148, 2455-9555 (2017).
- Nazari A, Riahi S, Riahi S, Shamekhi SF, Khademno A. Assessment of the effects of the cement paste composite in presence TiO₂ nanoparticles. J Am Sci, 6:43–6 (2010)
- Nazari A, Shadi R, Shirin R, Shamekhi SF, Khademno A. Improvement the mechanical properties of the cementitious composite by using TiO₂ nanoparticles. J Am Sci, 6:98–101 (2010).
- Nazari A, Riahi S. The effects of TiO₂ nanoparticles on properties of binary blended concrete. J Compos Mater;45:1181–8 (2011).
- Daniyal M, Akhtar S, Azam A. Effect of nano-TiO₂ on the properties of cementitious composites under different exposure environments. Journal of Materials Research and Technology. 8(6):6158-6172 (2019).
- Indian standard methods of sampling and analysis of concrete, IS 1199 (1959).
- Indian standard concrete mix proportioning – guidelines, IS 10262 (2009).
- Plain and Reinforced Concrete - Code of Practice, IS 456 (2000).
- V* P, T DF. X ray Diffraction (XRD) Analysis of Coir Pith Concrete. International Journal of Recent Technology and Engineering (IJRTE).8(5):717-719. (2020)
- Uzbas, B., & Aydin, A. C, Microstructural Analysis of Silica Fume Concrete with Scanning Electron Microscopy and X-Ray Diffraction. Engineering, Technology & Applied Science Research, 10(3) 5845–5850 (2020).
- T. G. N I J L A N D and J. A. LARBI1, Microscopic examination of deteriorated concrete, Non-Destructive Evaluation of Reinforced Concrete Structures, 137-179 (2010).

- [30] Elena Cerro-Prada, Cement Microstructure: Fostering Photocatalysis, Intech open, (2018).
- [31] Johansen V, Thaulow N, Skalny J. Simultaneous presence of alkali-silica gel and ettringite in concrete. *Advances in Cement Research*, 5(17) 23-9 (1993).
- [32] Fu Y, Xie P, Gu P, Beaudoin JJ. Preferred nucleation of secondary ettringite in preexisting cracks of steam cured cement paste. *J Mater Sci Lett*, 12(23) 1864-5 (1993).
- [33] Fu Y, Xie P, Gu P, Beaudoin JJ. Significance of preexisting cracks on nucleation of secondary ettringite in steam cured cement paste. *Cement Concrete Research*, 24(6) 1015-24 (1994).
- [34] Fu Y, Beaudoin JJ. Microcracking as a precursor to delayed ettringite formation in cement systems. *CemConcr Res* 26(10) 1493-8 (1996).
- [35] Tosun, K., & Baradan, B., Effect of ettringite morphology on DEF-related expansion. *Cement and Concrete Composites*, 32(4) 271-280 (2010).
- [36] Mielenz RO, Marusin SL, Hime WG, Jugovic ZT. Investigation of prestressed concrete railway tie distress. *Concrete International* 17(12) 62-8 (1995).